

Scale-free networks embedded in fractal space

K. Yakubo*

Department of Applied Physics, Hokkaido University, Sapporo 060-8628, Japan

D. Korošak†

*University of Maribor, Institute of Physiology, Faculty of Medicine, Maribor SI-2000, Slovenia and
University of Maribor, Faculty of Civil Engineering, Maribor SI-2000, Slovenia*

(Dated: November 22, 2021)

The impact of inhomogeneous arrangement of nodes in space on network organization cannot be neglected in most of real-world scale-free networks. Here, we propose a model for a geographical network with nodes embedded in a fractal space in which we can tune the network heterogeneity by varying the strength of the spatial embedding. When the nodes in such networks have power-law distributed intrinsic weights, the networks are scale-free with the degree distribution exponent decreasing with increasing fractal dimension if the spatial embedding is strong enough, while the weakly embedded networks are still scale-free but the degree exponent is equal to $\gamma = 2$ regardless of the fractal dimension. We show that this phenomenon is related to the transition from a non-compact to compact phase of the network and that this transition accompanies a drastic change of the network efficiency. We test our analytically derived predictions on the real-world example of networks describing the soil porous architecture.

PACS numbers:

I. INTRODUCTION

Scale-free organization of networks [1–3] seems to be the underlying principle common of many complex systems. In real-world networks, examples include the Internet, social networks or communication networks [4–9], the inhomogeneous arrangement of nodes in space strongly impacts the network organization and the linking rules must include the dependence on the distances between nodes [10–13]. However, most of the network models studied so far considered either randomly distributed nodes in metric space [14–17] or nodes placed on a lattice [18–22]. The importance of inhomogeneous spatial positions of nodes was emphasized in [4] where it was shown that the fractality of the space is one of the universal parameters that constrain the Internet models describing Internet’s large-scale topology and its observed scale-free character [23–25] at the router and autonomous system level. While preferential attachment [2, 3] seems to be the main underlying mechanism structuring the Internet, the original form of the preferential attachment [2] should be altered [4, 24, 26] to account for the observed spatial and/or functional heterogeneity of the nodes.

Here, we study the structure of networks formed by geographical network model in which the nodes with power-law distributed intrinsic weights (i.e., fitnesses [27–29]) are embedded in a fractal space. We show analytically that the networks produced by such model are scale-free with the degree exponent influenced by the fractal di-

mension of the embedding space if the spatial embedding is strong enough. By explicitly deriving the degree and the edge-length distribution functions, we classify these networks into non-compact phase with infinite average degree and average edge length and compact phase with finite average degree and average edge length, separated by an intermediate phase characterized by finite average degree and infinite average edge length. It is also shown that the transition between these phases accompanies a drastic change of the network efficiency. Finally, we use our findings in the analysis of the networks describing the soil porous architecture as an example.

II. MODEL

In order to describe an inhomogeneous distribution of N nodes in a space of linear dimension L , the nodes are isotropically distributed in a fractal manner with the fractal dimension D . In the theoretical treatment we employ an *artificial* boundary conditions for which every node position is statistically equivalent. This is slightly different from usual periodic boundary conditions leading to an anisotropy. The number of nodes is thus given by $N = \rho\Omega \int_0^L l^{D-1} dl$, where Ω is the D -dimensional solid angle and ρ is the density of nodes. Each node has a real and continuous fitness x randomly assigned according to the distribution function $s(x)$. If a node pair (i - j) satisfies

$$\frac{F(x_i, x_j)}{l_{ij}^m} > \Theta, \quad (1)$$

then these two nodes are connected by an edge, where l_{ij} is the Euclidean distance between the nodes i and j , m (≥ 0) is a real parameter quantifying the strength

*Electronic address: yakubo@eng.hokudai.ac.jp

†Electronic address: dean.korosak@uni-mb.si

of the spatial embedding (namely, the strength of the geographical effect), Θ is a threshold value, and $F(x, y)$ is a function relating the two fitnesses to the connectivity. If $m = 0$, we have a conventional fitness model which provides a scale-free network for a variety of combinations of forms of $F(x, y)$ and $s(x)$ [27, 28]. Here, we concentrate on the case of

$$F(x, y) = xy, \quad (2)$$

and

$$s(x) = s_0 x^{-\alpha}, \quad (3)$$

where x (and y) are in the range of $[x_{\min}, \infty)$ and $\alpha > 1$. From the normalization condition of $s(x)$, we have

$$s_0 = (\alpha - 1)x_{\min}^{\alpha-1}. \quad (4)$$

Similar geographical network models have been studied under the assumption that nodes are homogeneously distributed in a Euclidean space [16, 17], while here we investigate how the inhomogeneity (fractality) of spatial distribution of nodes affects properties of the network.

III. DEGREE DISTRIBUTION FUNCTION

First, we calculate the degree distribution function of the network formed by the above geographical algorithm.

Let $k_i(l)dl$ be the number of nodes connected to the node i and included in a thin spherical shell of the radius l (width dl) centered at the position of the node i . Since the distance between the node i and a node in the shell is l , the connectivity condition Eq. (1) tells us that nodes with $x_j > \Theta l^m/x_i$ can connect to the node i . Thus, the number of connected nodes $k_i(l)dl$ is

$$k_i(l)dl = n(l)dl \cdot \int_{\Theta l^m/x_i}^{\infty} s(x) dx, \quad (5)$$

where $n(l)dl = \rho\Omega l^{D-1}dl$ is the number of nodes in this spherical shell. In this expression, we assume that $\Theta l^m/x_j > x_{\min}$, which is equivalent to $l > l_{\min}(x_i)$ where

$$l_{\min}(x_i) = \left(\frac{x_{\min}x_i}{\Theta}\right)^{1/m}. \quad (6)$$

Nodes within the distance $l_{\min}(x_i)$ from the node i can connect to the node i . Thus, using Eq. (4), we have

$$k_i(l) = \begin{cases} \rho\Omega \left(\frac{x_{\min}}{\Theta}\right)^{\alpha-1} x_i^{\alpha-1} l^{D-1-m(\alpha-1)} & , l > l_{\min}(x_i), \\ \rho\Omega l^{D-1} & , l \leq l_{\min}(x_i). \end{cases} \quad (7a)$$

$$, l \leq l_{\min}(x_i). \quad (7b)$$

Integrating $k_i(l)$ with respect to l over $(0, L]$ we obtain the total number of nodes connected to the node i , or the degree k_i of the node i given by

$$k_i = \frac{\rho\Omega x_{\min}^{\alpha-1} L^{D-m(\alpha-1)}}{[D-m(\alpha-1)]\Theta^{\alpha-1}} x_i^{\alpha-1} + \frac{\rho\Omega x_{\min}^{D/m}}{\Theta^{D/m}} \left[\frac{1}{D} - \frac{1}{D-m(\alpha-1)} \right] x_i^{D/m}. \quad (8)$$

It should be noted that geometrical coefficients in two terms of Eq. (8) coming from the volume integration are not very meaningful for realistic systems because of our artificial boundary conditions. In the case of $D - m(\alpha - 1) > 0$, the first term of Eq. (8) dominates the second term when L is sufficiently large and we have $k_i \propto x_i^{\alpha-1}$. The degree distribution function $P(k)$ calculated from the relation $|P(k)dk| = |s(x)dx|$ is then proportional to k^{-2} independently of m , α , and D . If however, $D - m(\alpha - 1) \leq 0$, the second term of Eq. (8) becomes much

larger than the first term. The relation $k_i \propto x_i^{D/m}$ in this case leads to $P(k) \propto k^{-m(\alpha-1)/D+1}$. Therefore, the degree distribution function of the present geographical network model is given by

$$P(k) \propto \begin{cases} k^{-2} & , m \leq m_{c0}, \\ k^{-m(\alpha-1)/D+1} & , m > m_{c0}, \end{cases} \quad (9a)$$

$$, m > m_{c0}, \quad (9b)$$

where

$$m_{c0} = \frac{D}{\alpha - 1}. \quad (10)$$

The distribution function $P(k)$ obeys power-law forms in both cases of $m \leq m_{c0}$ and $m > m_{c0}$, and the degree exponent γ is

$$\gamma = \begin{cases} 2 & , m \leq m_{c0}, \\ \frac{m}{D}(\alpha - 1) + 1 & , m > m_{c0}. \end{cases} \quad (11)$$

The geographical inhomogeneity of the node distribution does not affect the degree distribution of the network for a weak geographical effect (small m), while γ depends on D for a strong effect (large m).

In the above argument, we assumed that the system size L is always larger than $l_{\min}(x_i)$ for any x_i , because we are interested in the thermodynamic case ($L \rightarrow \infty$). This is, however, not obvious, because x_i [and then $l_{\min}(x_i)$] can also diverge in the thermodynamic limit under a constant density ρ . Let us consider carefully this condition $L > l_{\min}(x_i)$. In a finite system with $N = \rho\Omega L^D/D$ nodes, the fitness x is truncated at a finite value. The maximum fitness x_{\max} is given by $N \int_{x_{\max}}^{\infty} s(x) dx = 1$. Using the fitness distribution Eq. (3) with Eq. (4), the quantity x_{\max} is given by

$$x_{\max} = N^{1/(\alpha-1)} x_{\min}. \quad (12)$$

Thus, the length $l_{\min}(x_i)$ can be as large as $l_{\min}(x_{\max})$, where

$$l_{\min}(x_{\max}) = \left[\frac{(\rho\Omega)^{1/(\alpha-1)} L^{D/(\alpha-1)} x_{\min}^2}{\Theta D^{1/(\alpha-1)}} \right]^{1/m}. \quad (13)$$

From the above expression, the condition $l_{\min}(x_{\max}) < L$ is equivalent to $\Theta > \Theta_0$, where

$$\Theta_0 = \left(\frac{\rho\Omega}{D} \right)^{\frac{1}{\alpha-1}} x_{\min}^2 L^{\frac{D}{\alpha-1} - m}. \quad (14)$$

If $m > m_{c0}$, the quantity Θ_0 goes to zero in the thermodynamic limit and any finite Θ satisfies $\Theta > \Theta_0$, namely, $l_{\min}(x_{\max}) < L$. Thus, the degree distribution function $P(k)$ is given by Eq. (9b) in the thermodynamic limit with $m > m_{c0}$. On the contrary, if $m \leq m_{c0}$, Θ is always less than Θ_0 because Θ_0 diverges as $L \rightarrow \infty$. In this case, there must be nodes satisfying $l_{\min}(x_i) > L$ for which $x_i > \Theta L^m/x_{\min}$. Since the condition $x_i > \Theta L^m/x_{\min}$ implies that any node in the whole system can connect to the node i , the degree of such a node is $N-1$ independent of x_i . Thus, these nodes give an additional δ -functional contribution $[\delta(k-N+1)]$ to the degree distribution $P(k)$ given by Eq. (9a) for nodes with $x_i < \Theta L^m/x_{\min}$. Let us estimate the magnitude of this δ -functional contribution. It is proportional to the number of nodes n_0 having $x_i > \Theta L^m/x_{\min}$. The quantity n_0 is given by $N \int_{\Theta L^m/x_{\min}}^{\infty} s(x) dx$ and can be written as

$$n_0 = N \left(\frac{L}{\xi} \right)^{-m(\alpha-1)}, \quad (15)$$

where ξ is the node-pair distance defined by

$$\xi = l_{\min}(x_{\min}) = \left(\frac{x_{\min}^2}{\Theta} \right)^{1/m}, \quad (16)$$

below which the two nodes are connected independently of the fitness. The properly normalized δ -functional part of $P(k)$ is then presented by $(L/\xi)^{-m(\alpha-1)} \delta(k-N+1)$.

Since $m(\alpha-1)$ is always positive, the δ -functional contribution vanishes in the thermodynamic limit. Therefore, Eq. (9) is valid both for the cases of $m \leq m_{c0}$ and $m > m_{c0}$ in an infinite system. For a finite L , however, Θ can be chosen to be less than Θ_0 independently of m and the δ -functional contribution remains finite. Thus, the degree distribution function of a finite system with $\Theta < \Theta_0$ must have the δ -functional correction term, that is,

$$P(k) = p_0 k^{-\gamma} + \left(\frac{L}{\xi} \right)^{-m(\alpha-1)} \delta(k-N+1), \quad (17)$$

for both $m \leq m_{c0}$ and $m > m_{c0}$. Here, p_0 is a normalization constant and the exponent γ is given by Eq. (11). It should be noted that Eq. (17) holds for a finite but large L because the first term of Eq. (17) is valid in the large L limit.

The quantity Θ_0 is a characteristic value of Θ peculiar to a finite system with a fixed density ρ . There are two other characteristic values of Θ for a finite L . One is Θ_{\min} below which every node can connect to all other $N-1$ nodes. Network constructed under $\Theta < \Theta_{\min}$ becomes the complete graph. Obviously, Θ_{\min} is given by

$$\Theta_{\min} = \frac{x_{\min}^2}{L^m}. \quad (18)$$

Another characteristic Θ is Θ_{\max} above which no node can connect to any other nodes. Network with $\Theta > \Theta_{\max}$ is a set of isolated nodes. We have

$$\Theta_{\max} = \frac{x_{\max}^2}{\Delta l^m}, \quad (19)$$

where $\Delta l = (\rho\Omega/D)^{-1/D}$ is the minimum edge length. Using Eq. (12), Θ_{\max} is written as

$$\Theta_{\max} = \left(\frac{\rho\Omega}{D} \right)^{\frac{2}{\alpha-1} + \frac{m}{D}} x_{\min}^2 L^{\frac{2D}{\alpha-1}}. \quad (20)$$

In a finite system we always assume that Θ satisfies the condition $\Theta_{\min} \ll \Theta \ll \Theta_{\max}$ leading to non-trivial networks. It is not necessary to consider this condition in an infinite system because Θ_{\min} and Θ_{\max} vanishes and diverges, respectively, in the thermodynamic limit.

IV. RELATION BETWEEN $\langle k \rangle$ AND Θ

From Eq. (9), it is clear that the average degree $\langle k \rangle$ diverges for $m \leq m_{c0}$ because of $\gamma = 2$ and it remains finite for $m > m_{c0}$ in the thermodynamic limit. The average degree $\langle k \rangle$ in a finite system is, however, always finite and depends on Θ . A large Θ restricts a connection of a node pair and leads a small $\langle k \rangle$. It is important to know the relation between Θ and $\langle k \rangle$ for a finite but large system. We calculate the average degree by

$$\langle k \rangle = \int_{x_{\min}}^{x_{\max}} k_i s(x) dx, \quad (21)$$

instead of $\langle k \rangle = \int kP(k)dk$, using the derived expression (not asymptotic form) of k_i for a finite system.

Let us consider Eq. (21) separately for $\Theta < \Theta_0$ and for $\Theta \geq \Theta_0$. In the case of $\Theta < \Theta_0$, the length $l_{\min}(x_i)$ can be larger than L , which implies $\Theta L^m/x_{\min} < x_{\max}$. Thus, the integral of Eq. (21) is separated into two regions

$$\langle k \rangle = \int_{x_{\min}}^{\Theta L^m/x_{\min}} k(x)s(x) dx + (N-1) \int_{\Theta L^m/x_{\min}}^{x_{\max}} s(x) dx, \quad (22)$$

where $k(x)$ is given by Eq. (8) regarding x_i as a continuous variable x . The coefficient $N-1$ in the second term comes from the fact that nodes satisfying $x_i > \Theta L^m/x_{\min}$ connect to all $N-1$ nodes. Using Eq. (8) and approximating $\int_{\Theta L^m/x_{\min}}^{x_{\max}} dx$ by $\int_{\Theta L^m/x_{\min}}^{\infty} dx$, we have

$$\begin{aligned} \langle k \rangle &= X\rho \left(\frac{x_{\min}^2}{\Theta} \right)^{\alpha-1} L^{D-m(\alpha-1)} \log \left(\frac{Y\Theta L^m}{x_{\min}^2} \right) \\ &\quad + Z\rho \left(\frac{x_{\min}^2}{\Theta} \right)^{D/m}, \end{aligned} \quad (23)$$

where

$$X = \frac{\Omega(\alpha-1)}{D-m(\alpha-1)}, \quad (24)$$

$$Y = \exp \left\{ \frac{d-2m(\alpha-1)}{(\alpha-1)[d-m(\alpha-1)]} \right\}, \quad (25)$$

$$Z = \frac{\Omega m^2(\alpha-1)^2}{D[D-m(\alpha-1)]^2}. \quad (26)$$

It should be again emphasized that these geometrical quantities X , Y , and Z resulting from the volume integration depend strongly on the boundary conditions and are not very meaningful. We can evaluate the asymptotic behavior of $\langle k \rangle$ for large L by using Eq. (23). In the case of $m < m_{c0}$, the first term of Eq. (23) obviously dominates the second term. Then, ignoring unimportant geographical coefficient, $\langle k \rangle$ behaves asymptotically as

$$\langle k \rangle \sim \Theta^{1-\alpha}(\log \Theta + c). \quad (27)$$

where c is a constant depending on the boundary condition. On the other hand, a careful treatment is required for $m > m_{c0}$. It seems that the second term of Eq. (23) dominates the first term for $m > m_{c0}$ in the thermodynamic limit. However, we should note that Θ must be infinitesimal to satisfy the condition $\Theta < \Theta_0$ in this calculation because Θ_0 for $L \rightarrow \infty$ goes to zero for $m > m_{c0}$ so it is not obvious which term is dominating in Eq. (23). In order to find the dominant term, we evaluate the lower bounds of these terms by replacing Θ by Θ_0 and using (14). Then, the lower bounds of the first and the second terms are proportional to $\log[Y(\rho\Omega/D)^{1/(\alpha-1)}L^{D/(\alpha-1)}]$ and $L^{[1-\frac{D}{m(\alpha-1)}]}$ respectively. This suggests that the second term dominates the first term for large L because the exponent $1-\frac{D}{m(\alpha-1)}$ is positive for $m > m_{c0}$. We have then

$$\langle k \rangle \sim \Theta^{-D/m}, \quad (28)$$

for $\Theta < \Theta_0$ and $m > m_{c0}$. At $m = m_{c0}$, both terms in Eq. (23) should be considered.

Next, we treat the case of $\Theta \geq \Theta_0$. Here $l_{\min}(x_i)$ is always less than L , and the degree k_i is given by Eq. (8) for any x_i in the range of $x_{\min} \leq x_i \leq x_{\max}$. The average degree $\langle k \rangle$ is then simply presented by

$$\begin{aligned} \langle k \rangle &= \int_{x_{\min}}^{x_{\max}} k(x)s(x) dx \\ &= \frac{\rho X}{\alpha-1} \left(\frac{x_{\min}^2}{\Theta} \right)^{\alpha-1} L^{D-m(\alpha-1)} \log(WL^D) \\ &\quad - \rho Z[D-m(\alpha-1)] \left(\frac{x_{\min}^2}{\Theta} \right)^{D/m} (WL^D)^{\frac{D}{m(\alpha-1)}-1} \\ &\quad + \rho Z[D-m(\alpha-1)] \left(\frac{x_{\min}^2}{\Theta} \right)^{D/m}, \end{aligned} \quad (29)$$

where $W = \rho\Omega/D$ and we used Eq. (8) for $k(x)$ and Eq. (12). For $m > m_{c0}$, it is easy to understand that the third term dominates other two terms for large L . So we have

$$\langle k \rangle \sim \Theta^{-D/m}. \quad (30)$$

In the case of $m < m_{c0}$, the infinitely large Θ must be considered when we find the dominant term of Eq. (29), because Θ is larger than Θ_0 and Θ_0 diverges for $m < m_{c0}$ in the thermodynamic limit. As in the case of $\Theta < \Theta_0$ and $m > m_{c0}$, replacing Θ in Eq. (29) by Θ_0 , the L dependence of the upper bounds of these terms points to the dominant term. Since the upper bounds of the first, second, and third terms are proportional to $\log(\rho\Omega L^D/D)$, L^0 , and $L^{D[1-\frac{1}{m(\alpha-1)}]}$, respectively, the first term dominates the second and third terms because of $m < m_{c0}$. Therefore, the average degree $\langle k \rangle$ is asymptotically given by

$$\langle k \rangle \sim \Theta^{1-\alpha}. \quad (31)$$

This relation differs from Eq. (27) by a logarithmic correction.

In summary, the relation between Θ and $\langle k \rangle$ is given by

$$\langle k \rangle \sim \begin{cases} \Theta^{1-\alpha}(\log \Theta + c) & , m < m_{c0} \\ \Theta^{-D/m} & , m > m_{c0} \end{cases} \quad (32a)$$

$$(32b)$$

for $\Theta < \Theta_0$ and

$$\langle k \rangle \sim \begin{cases} \Theta^{1-\alpha} & , m < m_{c0} \\ \Theta^{-D/m} & , m > m_{c0} \end{cases} \quad (33a)$$

$$(33b)$$

for $\Theta \geq \Theta_0$. At $m = m_{c0}$, $\langle k \rangle$ is related to Θ through Eq. (23) for $\Theta < \Theta_0$ and through Eq. (29) for $\Theta \geq \Theta_0$, because every term contributes equally to $\langle k \rangle$ even in the thermodynamic limit. A similar result to Eq. (33) has been obtained by [17] where the nodes were uniformly distributed in a d -dimensional space with the

L -max norm and m is fixed at $m = D(= d)$. The asymptotic L dependence of $\langle k \rangle$ for a fixed Θ can be also evaluated from Eqs. (23) and (29). In the case of $m < m_{c0}$ and enough large L (then, $\Theta < \Theta_0$), the dominant first term of Eq. (23) gives $\langle k \rangle \propto L^{D-m(\alpha-1)} \log L$. For $m > m_{c0}$ (and then $\Theta > \Theta_0$), we have $\langle k \rangle \propto L^0$. These L dependences are consistent with those calculated by $\langle k \rangle = \int_1^{N-1} kP(k) dk$ by using Eqs. (17) and (9b) for $m < m_{c0}$ and $m > m_{c0}$, respectively, and taking into account the L dependence of p_0 in Eq. (17).

V. EDGE-LENGTH DISTRIBUTION FUNCTION

In this section, we derive the edge-length distribution function $R(l)$ of our geographical networks embedded in a fractal space. To this end, we regard $k_i(l)$ given by Eq. (7) as a continuous function $k(x, l)$ of the fitness x and the edge length l . The average number of edges, $k(l)dl$, of length $[l, l + dl]$ from a given node is obtained by averaging $k(x, l)$ over the fitness x , i.e.,

$$k(l) = \int_{x_{\min}}^{x_{\max}} s(x)k(x, l) dx. \quad (34)$$

Equation (7) expresses the forms of $k_i(l)$ by separating two cases $l > l_{\min}(x_i)$ and $l \leq l_{\min}(x_i)$ for a fixed x_i . Corresponding to this classification, $k(x, l)$ in Eq. (34) for a fixed l has different forms for $x_{\min} \leq x < \Theta l^m/x_{\min}$ and $\Theta l^m/x_{\min} \leq x \leq x_{\max}$, respectively. Thus, the integral of Eq. (34) is calculated as

$$k(l) = \rho\Omega \left(\frac{x_{\min}}{\Theta}\right)^{\alpha-1} l^{D-1-m(\alpha-1)} \int_{x_{\min}}^{x_l} s(x)x^{\alpha-1} dx + \rho\Omega l^{D-1} \int_{x_l}^{\infty} s(x) dx, \quad (35)$$

where $x_l = \Theta l^m/x_{\min}$. Here, l is assumed to be larger than ξ (namely, $x_{\min} < x_l$) and the upper cut-off of the integral is, as an approximation, extended to infinity. Using Eqs. (3), (4), (7), and (16), $k(l)$ is expressed by

$$k(l) = \rho\Omega l^{D-1} \left(\frac{l}{\xi}\right)^{-m(\alpha-1)} \left[1 + m(\alpha-1) \log\left(\frac{l}{\xi}\right)\right]. \quad (36)$$

The probability distribution function $R(l)$ is given by

$$R(l) = \frac{k(l)}{\int_L k(l') dl'}, \quad (37)$$

where the integration in the denominator is done over the whole range of l . Neglecting the normalization constant, the edge-length distribution is

$$R(l) \propto l^{D-1} \left(\frac{l}{\xi}\right)^{-m(\alpha-1)} \left[1 + m(\alpha-1) \log\left(\frac{l}{\xi}\right)\right]. \quad (38)$$

We should remark that $R(l)$ for $m \leq m_{c0}$ goes to infinity as $l \rightarrow \infty$. Since the length l does not exceed the size L in a finite system, the distribution $R(l)$ is actually truncated at $l = L$. In the thermodynamic limit, however, we must consider the infinitesimal normalization constant coming from the denominator of Eq. (37).

In the case of $l \leq \xi$ (namely, $x_{\min} \geq x_l$), $k(x, l)$ in Eq. (34) is given by Eq. (7b) for any x in the integration range $[x_{\min}, x_{\max}]$. Thus, $k(l)$ is given by $\rho\Omega l^{D-1} \int_{x_{\min}}^{\infty} s(x) dx$, namely,

$$k(l) = \rho\Omega l^{D-1}, \quad (39)$$

and then,

$$R(l) \propto l^{D-1}. \quad (40)$$

It should be noted that the distribution $R(l)$ depends on the fractal dimension D independently of m while the degree distribution $P(k)$ does not depend on D for $m \leq m_{c0}$ (weak geographical effect region).

Two expressions Eqs. (38) and (40) of $R(l)$ for $l > \xi$ and $l \leq \xi$ must coincide at $l = \xi$. This condition concludes that the proportionality coefficients for Eqs. (38) and (40) are identical. We can derive the common coefficient C for an infinite system from the normalization condition of $R(l)$ given by

$$1 = C \int_0^{\xi} l^{D-1} dl + C \int_{\xi}^{\infty} l^{D-1} \left(\frac{l}{\xi}\right)^{-\beta} \left[1 + \beta \log\left(\frac{l}{\xi}\right)\right] dl, \quad (41)$$

where $\beta = m(\alpha-1)$. When $m > m_{c0}$, this equation provides a finite coefficient expressed by

$$C = \frac{D}{\xi^D} \left(1 - \frac{m_{c0}}{m}\right)^2, \quad (42)$$

while C is infinitesimal for $m \leq m_{c0}$ as mentioned above. It should be noted that the coefficient C does not depend on the boundary condition because the boundary-condition dependent factors in the numerator and the denominator in Eq. (37) are canceled out.

From the above argument, we can immediately derive the probability $g(l)$ of two nodes with distance l to be connected. This probability is given by the ratio of the number of connected nodes $k(l)dl$ to $n(l)dl$ nodes located at distances $[l, l + dl]$ from a given node, namely, $g(l) = k(l)/n(l)$. Since $n(l) = \rho\Omega l^{D-1}$ as mentioned below Eq. (5) and $k(l)$ is given by Eq. (36) or (39) for $l > \xi$ or $l \leq \xi$ respectively, we have

$$g(l) = \begin{cases} \left(\frac{l}{\xi}\right)^{-m(\alpha-1)} \left[1 + m(\alpha-1) \log\left(\frac{l}{\xi}\right)\right] & , l > \xi, \\ 1 & , l \leq \xi. \end{cases} \quad (43)$$

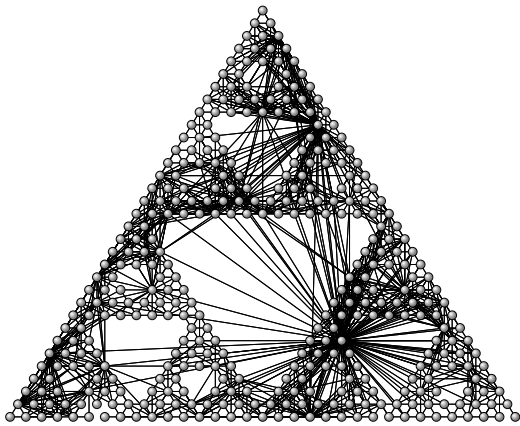


FIG. 1: Typical Sierpinski geographical network. Nodes are located on vertices of the Sierpinski gasket in the 6th generation ($N = 366$). Parameters to form the network are $\alpha = 2.0$ and $m = 3.0$. The threshold Θ is chosen to satisfy $\langle k \rangle = 10.0$.

This expression can be alternatively derived directly from the meaning of $g(l)$,

$$g(l) = \int_{x_{\min}}^{\infty} s(x)dx \int_{xy/l^m > \Theta} s(y)dy . \quad (44)$$

Considering that two nodes are always connected if the fitness of one node exceeds $x_l (= \Theta l^m / x_{\min})$, we can separate the above integration into two parts as

$$g(l) = \int_{x_l}^{\infty} s(x)dx + \int_{x_{\min}}^{x_l} s(x)dx \int_{\Theta l^m / x}^{\infty} s(y)dy , \quad (45)$$

for $x_l > x_{\min}$ ($l > \xi$). For $x_l \leq x_{\min}$, the integral range of the second integral in Eq. (44) is spread over the whole region of y , then $g(l) = \int_{x_{\min}}^{\infty} \int_{x_{\min}}^{\infty} s(x)s(y)dx dy$. These equations again lead Eq. (43) if we use Eq. (3). We should note that the probability $g(l)$ given by Eq. (43) does not depend on the fractal dimension D for any value of m .

VI. NUMERICAL CONFIRMATIONS

The above analytical results are numerically verified in this section. At first, we confirm the behavior of the degree distribution function $P(k)$ for geographical networks on the Sierpinski node set (Sierpinski geographical networks). Nodes are located on vertices of the Sierpinski gasket with the fractal dimension $D = \log 3 / \log 2 \approx 1.585$ and connected by edges according to the condition Eq. (1) with Eqs. (2) and (3). In our numerical calculations in this work, the lower cut-off x_{\min} is set to be unity. A typical network on the 6th generation Sierpinski gasket ($N = 366$) is depicted in Fig. 1. There exist nodes (hubs) possessing a large number of edges. Numerically calculated degree distribution functions $P(k)$ for two networks with different m and α are presented in Fig. 2. The scale-free property of networks formed by our algorithm

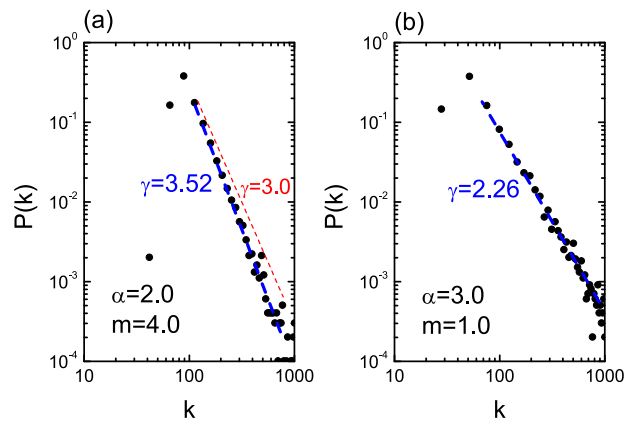


FIG. 2: (Color online) Degree distribution of Sierpinski geographical networks in the 9th generation ($N = 9,843$). The threshold Θ is chosen to satisfy $\langle k \rangle = 120.0$ for good statistics. Parameters α and m are set as (a) $\alpha = 2.0$ and $m = 4.0$ and (b) $\alpha = 3.0$ and $m = 1.0$. Thick dashed lines through dots indicate the slopes γ predicted by Eq. (11). Thin dashed line in Fig. 2(a) represents the slope calculated by using the Euclidean dimension $d = 2$ instead of the fractal dimension $D = 1.585$.

is clearly shown in this figure. The scale-free exponents γ calculated numerically for many Sierpinski geographical networks with different combinations of α and m are plotted in Fig. 3 as a function of $m(\alpha - 1)/D$. In this figure, values of γ for networks with nodes distributed homogeneously in two-dimensional Euclidean space (2d-geographical networks) are also plotted. We should remark that our theoretical arguments are valid for a geographical network with homogeneously distributed nodes which is a special case with the Euclidean dimension d

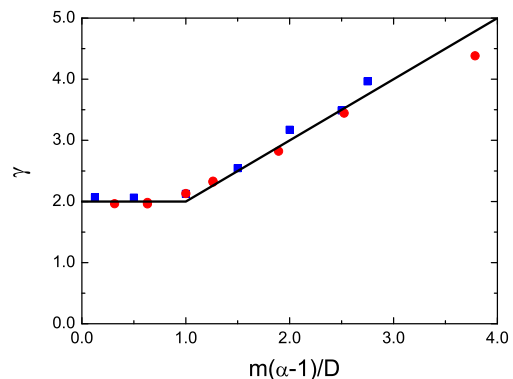


FIG. 3: (Color online) Degree exponent γ as a function of $m(\alpha - 1)/D$. Solid line shows the theoretical prediction Eq. (11). Filled circles and squares represent numerically obtained γ for Sierpinski geographical networks (9th generation) and 2d-geographical networks ($N = 1,000$) with several combinations of α and m . Values of γ are evaluated by the least-squares fit.

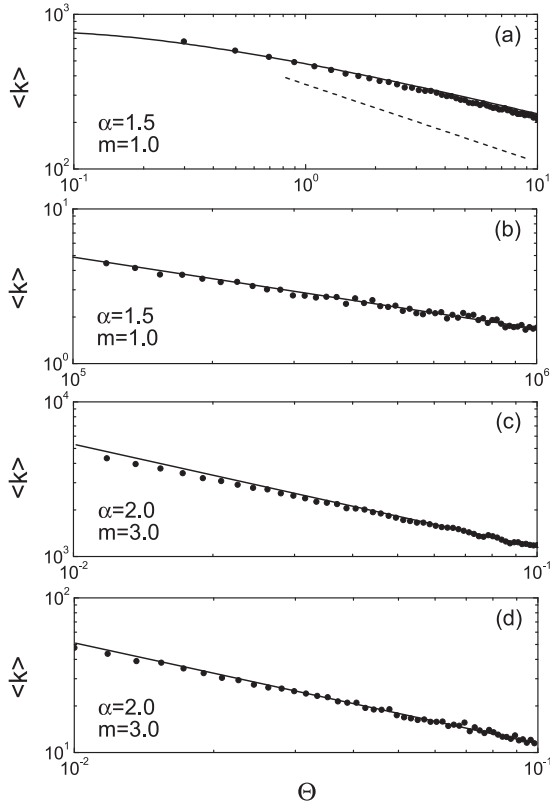


FIG. 4: Relation between the average degree $\langle k \rangle$ and the threshold value Θ for (a) $m < m_{c0}$ and $\Theta < \Theta_0$, (b) $m < m_{c0}$ and $\Theta > \Theta_0$, (c) $m > m_{c0}$ and $\Theta < \Theta_0$, and (d) $m > m_{c0}$ and $\Theta > \Theta_0$. Dots represent results calculated numerically for 2d-geographical networks. Details of parameters and conditions are given in the text. Solid curves show the theoretical predictions given by Eqs. (32) and (33). Dashed line in Fig. 4(a) indicates the slope given by Eq. (32a) without the logarithmic term.

instead of the fractal dimension D . In fact, Eq. (11) with $D = d$ reproduces the results by [16, 17]. We see that all numerical results collapse onto the theoretical line given by Eq. (11). These results strongly support the theoretical predictions on $P(k)$ presented in Sec. III.

Next, we confirm numerically the relation between $\langle k \rangle$ and Θ for 2d-geographical networks. We have to evaluate Θ_0 defined by Eq. (14) to distinguish four regions with respect to m and Θ corresponding to Eqs. (32) and (33). In addition, Θ must satisfy the condition $\Theta_{\min} \ll \Theta \ll \Theta_{\max}$, where Θ_{\min} and Θ_{\max} are given by Eqs. (18) and (20), respectively. Rewriting Eqs. (14) and (20) by $\Theta_0 = N^{1/(\alpha-1)} x_{\min}^2 L^{-m}$ and $\Theta_{\max} = N^{[2D+m(\alpha-1)]/[D(\alpha-1)]} x_{\min}^2 L^{-m}$, we can estimate Θ_0 and Θ_{\max} without treating the boundary-condition dependent geometrical factor $\rho\Omega/D$. Figures 4(a) and 4(b) show numerically calculated $\langle k \rangle$ as a function of Θ for $m < m_{c0}$. In these calculations, the exponent m characterizing the strength of the geographical effect are chosen to be 1.0, and $N = 1,000$ nodes are distributed in a square of size $L = 100.0$. The fitness x is allocated

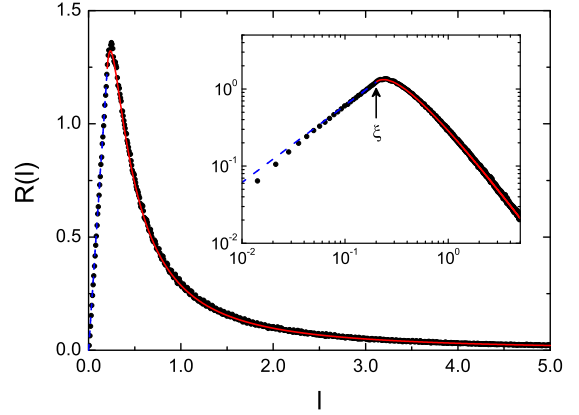


FIG. 5: (Color online) Edge-length distribution function $R(l)$ for 2d-geographical networks in squares of size $L = 10.0$. In order to obtain the numerical results (dots), we employ $\alpha = 2.0$ ($m_{c0} = 2.0$), $m = 3.0$, and $N = 1,000$. The threshold value Θ is chosen as $\Theta = 125.2$ so that $\langle k \rangle$ becomes equal to 10.0. The results are averaged over 1,000 realizations. Solid and dashed lines represent the theoretical results given by Eq. (38) and (40) with the common prefactor presented by Eq. (42). The inset shows the same result in a logarithmic scale. The length $\xi (= 0.20)$ defined by Eq. (16) is indicated by the arrow.

to each node according to the distribution function $s(x)$ given by Eq. (3) with $\alpha = 1.5$. The square system has the periodic boundary conditions in the x and y directions. Since $m_{c0} = 4.0$, $\Theta_0 = 10^4$, $\Theta_{\min} = 0.01$, and $\Theta_{\max} = 3.2 \times 10^{11}$ from these parameters, the conditions $\Theta_{\min} \ll \Theta < \Theta_0 \ll \Theta_{\max}$ and $\Theta_{\min} \ll \Theta < \Theta \ll \Theta_{\max}$ are satisfied for Figs. 4(a) and 4(b), respectively, and $m < m_{c0}$ for both figures. Numerically calculated $\langle k \rangle$ s are well described by solid lines representing Eqs. (32a) and (33a), where the constant c in Eq. (32a) and prefactors are suitably chosen. Results for $m > m_{c0}$ are presented in Figs. 4(c) and 4(d) which show the $\langle k \rangle$ - Θ relation for $\Theta < \Theta_0$ and $\Theta > \Theta_0$, respectively. As in the cases of Figs. 4(a) and 4(b), nodes are distributed in a square of size $L = 100.0$. Parameters α and m are chosen as $\alpha = 2.0$ and $m = 3.0$ so that the condition $m > m_{c0} (= 2.0)$ is satisfied. In order to realize the condition $\Theta_{\min} \ll \Theta < \Theta_0 \ll \Theta_{\max}$ in Fig. 4(c), we treated a large network with $N = 100,000$, which has $\Theta_{\min} = 10^{-6}$, $\Theta_{\max} = 3.2 \times 10^{11}$, and $\Theta_0 = 0.1$. On the contrary, the number of nodes for Fig. 4(d) is $N = 1,000$, in which $\Theta_{\min} \ll \Theta_0 < \Theta \ll \Theta_{\max}$ is satisfied with $\Theta_{\min} = 10^{-6}$, $\Theta_{\max} = 3.2 \times 10^4$, and $\Theta_0 = 0.001$. Similarly to Figs. 4(a) and 4(b), numerical results agree well with the theoretical results shown by solid lines.

Finally, the behavior of the edge-length distribution function $R(l)$ is examined also for 2d-geographical networks. Results (dots) shown in Fig. 5 are calculated in the condition of $m > m_{c0}$, for which $R(l)$ can be properly normalized even in the thermodynamic limit. Solid and

TABLE I: Three phases of geographical networks embedded in a fractal space.

Phase	Region of m	$\langle k \rangle$	$\langle l \rangle$
Non-compact	$m \leq m_{c0}$	infinite	infinite
Intermediate	$m_{c0} < m \leq m_{c1}$	finite	infinite
Compact	$m > m_{c1}$	finite	finite

dashed curves represent the theoretical prediction given by Eq. (38) and (40) with the common prefactor presented by Eq. (42). It should be emphasized that there is no fitting parameter to obtain the theoretical curve. Numerical results agree quite well with the theoretical prediction. The peak structure and the tail profile slightly deviating from a power law (see the inset of Fig. 5) result from the logarithmic term of Eq. (38). The reason of the slight deviation between numerical results and the theoretical line for $l \lesssim 0.05$ (see the inset) is due to a finite Δl defined below Eq. (19).

VII. COMPACTNESS AND EFFICIENCY

From the functional forms of $P(k)$ and $R(l)$, we can immediately find the convergence property of the average degree $\langle k \rangle$ and the average edge length $\langle l \rangle$ in the thermodynamic limit. As argued at the end of Sec. IV, the quantity $\langle k \rangle$ for $m \leq m_{c0}$ diverges as $L^{D-m(\alpha-1)} \log L$ and it converges for $m > m_{c0}$. On the other hand, the convergence of $\langle l \rangle$ is governed by Eq. (38) describing $R(l)$ in the asymptotic l regime. From Eq. (38), the average $\langle l \rangle$ diverges for $m \leq m_{c1}$ and remains finite for $m > m_{c1}$, where

$$m_{c1} = \frac{D+1}{\alpha-1}. \quad (46)$$

The behavior of $\langle k \rangle$ and $\langle l \rangle$ suggests that the impact of the geographical effect can be classified into three regions. For $0 \leq m \leq m_{c0}$, both quantities $\langle k \rangle$ and $\langle l \rangle$ diverge in the thermodynamic limit. Since a node connects with a huge number of nodes far away we call this region the *non-compact phase*. In the same sense, the region of $m > m_{c1}$ is termed the *compact phase* where both quantities $\langle k \rangle$ and $\langle l \rangle$ remain finite and a node connects with only a small number of nodes in its vicinity. In the *intermediate phase*, i.e., $m_{c0} < m \leq m_{c1}$, the average degree converges but $\langle l \rangle$ diverges. These regions are summarized in Table I.

Let us consider the relation between the compactness of a network and the geographical efficiency e defined by

$$e = \frac{2}{N(N-1)} \sum_{i>j} \frac{1}{r_{ij}}, \quad (47)$$

where r_{ij} is the shortest Euclidean distance between two nodes i and j along a network path. This quantity is a

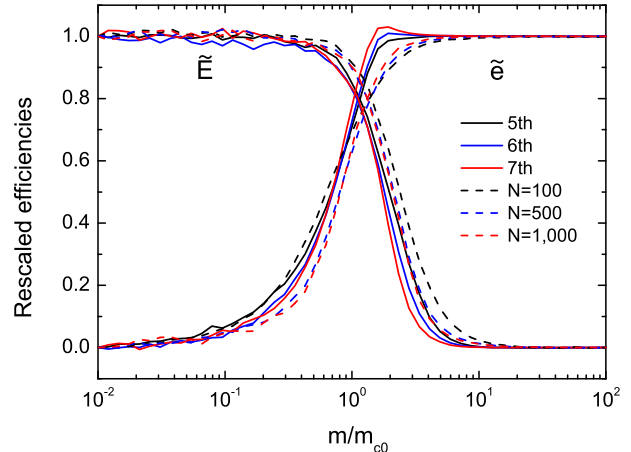


FIG. 6: (Color online) Rescaled geographical and global efficiencies as a function of m/m_{c0} for Sierpinski (solid lines) and 2d- (dashed lines) geographical networks. For both network systems, we employ $\alpha = 2.0$ and Θ giving $\langle k \rangle = 10.0$, and all results are averaged over 1,000 realizations. Numbers of nodes in Sierpinski geographical networks in the 5th, 6th, and 7th generations are 123, 336, and 1,095, respectively.

natural extension of the global efficiency E defined by

$$E = \frac{2}{N(N-1)} \sum_{i>j} \frac{1}{d_{ij}}, \quad (48)$$

where d_{ij} is the shortest network distance between two nodes i and j introduced in [30]. Both quantities e and E characterize the efficiency of the information exchange or the flow in the network. If the efficiency is governed mainly by the Euclidean distance along the path rather than the number of steps, the geographical efficiency e is more meaningful than E , and vice versa.

We calculated numerically these quantities and examined how the compactness is related to the efficiencies e and E . Solid lines in Fig. 6 represent the efficiencies for Sierpinski geographical networks in three different generations (having the same linear dimension $L = 1.0$), while dashed lines show them for 2d-geographical networks with different numbers of nodes in squares of size $L = 10.0$. In order to eliminate the L and N dependence of the maximum and minimum values of the efficiencies, we plot the rescaled quantities \tilde{e} and \tilde{E} defined by $\tilde{e} = (e - e_{\min})/(e_{\max} - e_{\min})$ and $\tilde{E} = (E - E_{\min})/(E_{\max} - E_{\min})$, where e_{\min} (E_{\min}) and e_{\max} (E_{\max}) are e (E) at $m/m_{c0} = 10^{-2}$ and 10^2 , respectively. The rescaled geographical (global) efficiency \tilde{e} (\tilde{E}) rapidly increases (decreases) near $m = m_{c0}$ as increasing m . From the fact that enlarging the system the slope near $m = m_{c0}$ becomes steeper and the point at the intersection of \tilde{e} and \tilde{E} approaches $m = m_{c0}$, the efficiencies e and E in the thermodynamic limit are supposed to show step-like forms at $m = m_{c0}$. This behavior

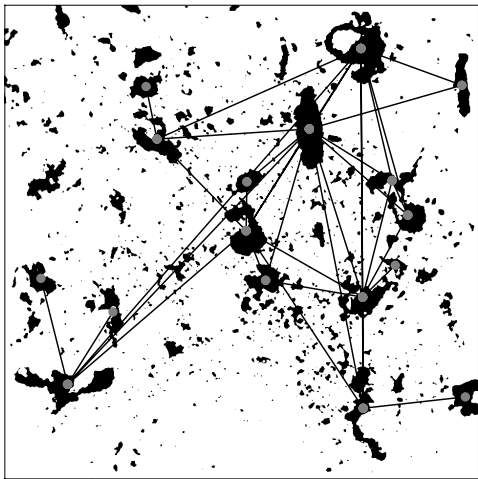


FIG. 7: 2d X-ray CT image of a soil structure with network edges connecting pores (black patches) according to Eq. (1) with $m = 5$ and $\Theta = 0.01$. From [31].

can be interpreted as follows. In the non-compact phase ($m < m_{c0}$), existing short-cut edge (in the topological sense) connects a starting node and a target node by a small number of edges with going back-and-forth around the target node. This back-and-forth motion, however, requires an extra Euclidean distance and leads the low geographical efficiency. On the other hand, in the compact phase, the network structure resembles the structure of a regular lattice (or regular Sierpinski gasket). Although we need lots of edges to connect two distant nodes, the total Euclidean length along the path can be minimized as the geodesic distance between two nodes. Thus, the geographical efficiency e becomes large in this region. The above consideration supports that the global efficiency E measuring the number of edges to connect nodes is large for $m < m_{c0}$ and small for $m > m_{c0}$. It should be noted that the abrupt change in e or E occurs at $m = m_{c0}$ but not at $m = m_{c1}$ though the transition point m_{c1} is related to the edge length. Since e and E behave oppositely, it is crucial to clarify which efficiency is more relevant to a given problem by considering how strongly the cost of the flow is influenced by the Euclidean distance. It is also interesting that both efficiencies e and E are relatively high in the network at $m = m_{c0}$ at which the competition between order and disorder in the geometrical sense is balanced.

VIII. EXAMPLE

We will demonstrate the above described approach using soil-pore networks as an example of a real-world spatially embedded network. Two approaches to build complex network models of soil-pore organization have recently been developed [31–33]. Here, we will concentrate on the networks presented in [31] formed by geographical threshold algorithm as described in Sec. II. We consider

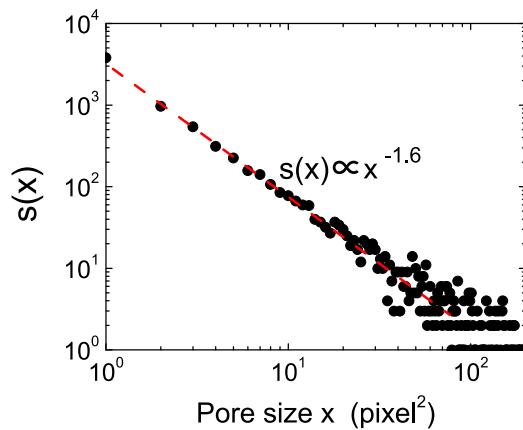


FIG. 8: (Color online) Pore-size distribution obtained from the image analysis of the soil structure shown in Fig. 7. Dashed line shows the power-law fit $s(x) \sim x^{-\alpha}$ to the distribution with $\alpha = 1.6$.

a set of N pores representing the nodes of the network. The nodes of the network are the centers of the pores and the links between nodes are drawn according to Eq. (1) with Eqs. (2) and (3), where in this case the continuous fitness variable x is the size of the pore. Pore sizes and their relative positions of actual soil specimens are obtained from the image analysis of 2d soil X-CT scans [31].

An example of the soil-pore network overlain on the 2d soil porous structure image is presented in Fig. 7 (from [31]). The pore-size distribution of the soil sample shown in Fig. 7 is analyzed to be of the form $s(x) \sim x^{-\alpha}$ with $\alpha = 1.6$ (Fig. 8). The fractal dimension $D = 1.32$ of the soil-pore structure is also determined using box-counting method as shown in Fig. 9. Our theory predicts that

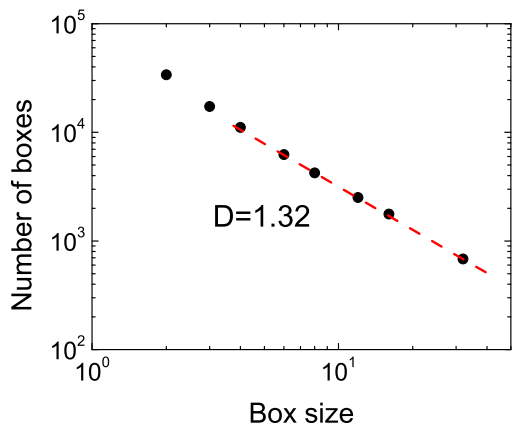


FIG. 9: (Color online) Number of boxes required to cover the soil-pore image shown in Fig. 7 as a function of the box size. The slope obtained by the least-squares fit (dashed line) indicates that the fractal dimension of the soil-pore structure is 1.32.

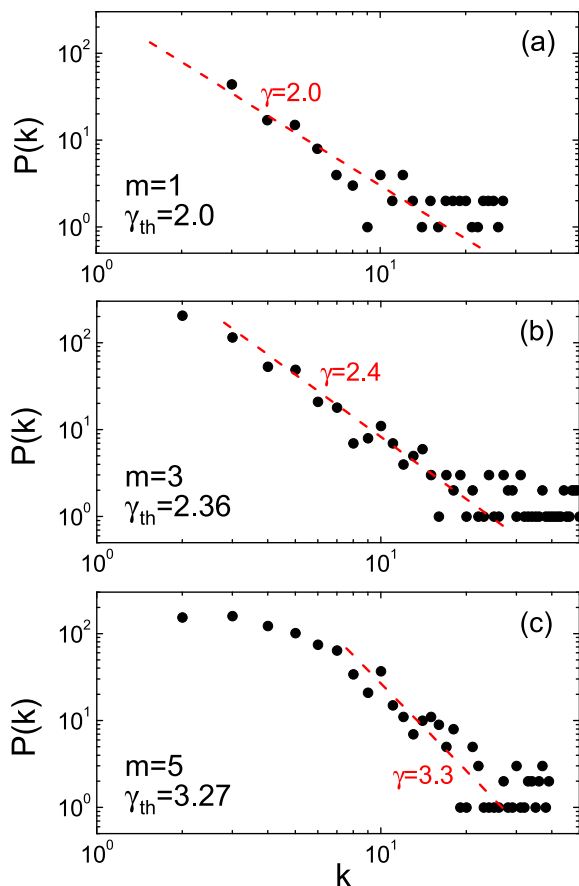


FIG. 10: (Color online) Degree distributions for three soil-pore networks formed by (a) $m = 1$, (b) $m = 3$, and (c) $m = 5$. Dashed lines through dots represent the power-law fits with the slopes indicated beside the lines. γ_{th} in each panel gives the degree exponent predicted by Eq. (11) with $D = 1.32$ and $\alpha = 1.6$.

the soil-pore network has a power-law degree distribution function and the degree exponent γ depends on m above $m_{c0} = 2.2$. Figure 10 shows the degree distributions for three networks based on soil image data constructed with different values of the parameter m ($m = 1, 3$, and 5). In this figure, the power-law fits (dashed lines) and calculated exponents of the degree distributions are shown together with theoretically predicted scale-free exponents from Eq. (11). The results clearly demonstrate the agreement of the empirically obtained scale-free exponents and the theoretically predicted ones. This also shows how the

fractality of pore spatial distribution is reflected in the network organization. By measuring the scaling exponent γ of the degree distribution for any $m > m_{c0}$ and the exponent α of the pore-size distribution, the fractal dimension D can be determined.

IX. CONCLUSIONS

We have proposed a geographical scale-free network model with the nodes embedded in a fractal space and analytically and numerically studied several network properties. The fractal dimension D of the embedding space was found to influence the scale-free exponent as $\gamma = m(\alpha - 1)/D + 1$ only if the spatial embedding is strong enough (i.e., when $m > m_{c0}$) otherwise $\gamma = 2$. The analyses of the average degree and average edge length revealed that this type of network can exist either in the non-compact, compact, or intermediate phase depending on the importance of the spatial arrangement of nodes. We derived the edge-length distribution functions for our network model and showed that it has a peak-like structure similar to the profile of the shortest-path-distance distribution observed in a large-scale structure of the Internet [24, 34]. It is interesting to apply our approach to modeling the Internet at the autonomous systems level considering the observed long-tailed distribution of autonomous systems sizes [35]. The measured degree distribution exponent of the Internet is slightly larger than $\gamma = 2$ ($\gamma = 2.1 \sim 2.2$) [24, 25] and seems to be decreasing with time [25]. In our network model this would be an indication of the evolution of the Internet towards the non-compact phase ($m \rightarrow m_{c0}$).

We hope that our work will help in advancing the understanding of the complex systems in which the heterogeneity of intrinsic properties and the spatial arrangement of the elements play an important role.

Acknowledgments

This work was supported in part by a Grant-in-Aid for Scientific Research (No. 22560058) from Japan Society for the Promotion of Science and by grant No. J3-2290 from Slovenian Research Agency. Numerical calculations in this work were performed on the facilities of the Supercomputer Center, Institute for Solid State Physics, University of Tokyo.

-
- [1] A.-L. Barabasi, *Science* **325**, 412 (2009).
 - [2] A.-L. Barabasi and R. Albert, *Science* **286**, 509 (1999).
 - [3] R. Albert and A.-L. Barabasi, *Rev. Mod. Phys.* **74**, 47 (2002).
 - [4] S.-H. Yook, H. Jeong, and A.-L. Barabasi, *Proc. Natl. Acad. Sci. U.S.A.* **99**, 13382 (2002).
 - [5] S. Eubank, H. Guclu, V. S. A. Kumar, M. V. Marathe,

- A. Srinivasan, Z. Toroczkai, and N. Wang, *Nature* **429**, 180 (2004).
- [6] D. Liben-Nowell, J. Novak, R. Kumar, P. Raghavan, and A. Tomkins, *Proc. Natl. Acad. Sci. U.S.A.* **102**, 11623 (2005).
- [7] M. T. Gastner and M. E. J. Newman, *Eur. Phys. J. B* **49**, 247 (2006).

- [8] R. Lambiotte, V. D. Blondel, C. de Kerchove, E. Huens, C. Prieur, Z. Smoreda, and P. Van Doorena, *Physica A* **387**, 5317 (2008).
- [9] G. Bianconi, P. Pin, and M. Marsili, *Proc. Natl. Acad. Sci. U.S.A.* **106**, 11433 (2009).
- [10] R. Xulvi-Brunet and I. M. Sokolov, *Phys. Rev. E* **66**, 026118 (2002).
- [11] M. Barthelemy, *Europhys. Lett.* **63**, 915 (2003).
- [12] M. Kaiser and C. C. Hilgetag, *Phys. Rev. E* **69**, 036103 (2004).
- [13] R. Xulvi-Brunet and I. M. Sokolov, *Phys. Rev. E* **75**, 046117 (2007).
- [14] J. Dall and M. Christensen, *Phys. Rev. E* **66**, 016121 (2002).
- [15] C. Herrmann, M. Barthelemy, and P. Provero, *Phys. Rev. E* **68**, 26128 (2003).
- [16] N. Masuda, H. Miwa, and N. Konno, *Phys. Rev. E* **71**, 036108 (2005).
- [17] S. Morita, *Phys. Rev. E* **73**, 035104 (2006).
- [18] J. M. Kleinberg, *Nature* **406**, 845 (2000).
- [19] C. P. Warren, L. M. Sander, and I. M. Sokolov, *Phys. Rev. E* **66**, 056105 (2002).
- [20] A. F. Rozenfeld, R. Cohen, D. ben-Avraham, and S. Havlin, *Phys. Rev. Lett.* **89**, 218701 (2002).
- [21] D. ben-Avraham, A. F. Rozenfeld, R. Cohen, and S. Havlin, *Physica A* **330**, 107 (2003).
- [22] K. Kosmidis, S. Havlin, and A. Bunde, *Europhys. Lett.* **82**, 48005 (2008).
- [23] M. Faloutsos, P. Faloutsos, and C. Faloutsos, *Comput. Commun. Rev.* **29**, 251 (1999).
- [24] A. Vazquez, R. Pastor-Satorras, and A. Vespignani, *Phys. Rev. E* **65**, 066130 (2002).
- [25] G. Siganos, M. Faloutsos, P. Faloutsos, and C. Faloutsos, *IEEE-ACM Trans. Netw.* **11**, 514 (2003).
- [26] S. Shakkottai, M. Fomenkov, R. Koga, D. Krioukov, and K. C. Claffy, *Eur. Phys. J. B* **74**, 271 (2010).
- [27] G. Caldarelli, A. Capocci, P. De Los Rios, and M. A. Munoz, *Phys. Rev. Lett.* **89**, 258702 (2002).
- [28] N. Masuda, H. Miwa, and N. Konno, *Phys. Rev. E* **70**, 36124 (2004).
- [29] D. Garlaschelli, A. Capocci, and G. Caldarelli, *Nature Physics* **3**, 813 (2007).
- [30] V. Latora and M. Marchiori, *Phys. Rev. Lett.* **87**, 198701 (2001).
- [31] S. J. Mooney and D. Korošak, *Soil Sci. Soc. Am. J.* **73**, 1094 (2009).
- [32] A. Santiago, J. P. Cardenas, J. C. Losada, R. M. Benito, A. M. Tarquis, and F. Borondo, *Nonlin. Processes Geophys.* **15**, 893 (2008).
- [33] J. P. Cardenas, A. Santiago, A. M. Tarquis, J. C. Losada, F. Borondo, and R. M. Benito, *Geoderma*, doi:10.1016/j.geoderma.2010.04.024 (in press).
- [34] P. Mahadevan, D. Krioukov, M. Fomenkov, B. Huffaker, X. Dimitropoulos, K. Claffy, and A. Vahdat, *Comput. Commun. Rev.* **36**, 17 (2006).
- [35] A. Lakhina, J. W. Byers, M. Crovella, and I. Matta, *IEEE J. Sel. Areas Commun.* **21**, 934 (2003).